agriculture

MDPI

Article

Development of a Cutting Machine for Hybrid Rice Male Parents in Narrow-Row Agriculture: Design, Simulation, and Validation

Ranbing Yang [1,2,3], Hao Zhang [1,2,3], Wanru Liu [1,2,3,*], Yiren Qing [1,2], Jian Zhang [1,2,3], Xiantao Zha [1,3] and Zhuxin Xu [4]

[1] School of Mechanical and Electrical Engineering, Hainan University, Haikou 570228, China; zhlovewave@gmail.com (H.Z.)
[2] School of Breeding and Multiplication (Sanya Institute of Breeding and Multiplication), Hainan University, Sanya 572000, China
[3] Key Laboratory of Tropical Intelligent Agricultural Equipment, Ministry of Agriculture and Rural Affairs, Danzhou 571700, China
[4] Qingdao Plantech Mechanical Technology Co., Ltd., Qingdao 266109, China
* Correspondence: 997309@hainanu.edu.cn; Tel.: +86-18595850940

Abstract

To address seed contamination, narrow-row mechanized cutting difficulties, and potential damage to maternal plants in muddy paddy fields during hybrid rice seed production, a walk-behind self-propelled hybrid rice male parent pulverizing and cutting machine was designed. The machine primarily consists of three key structures: a key cutting device, a gravity-free crop dividing device, and a crawler walking mechanism. The cutting device features an innovative mechanism where main-shaft rotation drives flail blades into inertial autorotation, while a stopper bar physically constrains their maximum swing amplitude to guarantee a 500 mm working width. Crucially, the gravity-free crop dividing device safely pushes aside adjacent maternal plants to effectively prevent accidental mechanical injury. A flexible plant model and a kinematic model were established using DEM software EDEM 2024. A three-factor, three-level orthogonal experiment indicated that the primary order of influence on the male parent cutting rate is forward speed > flail-blade rotational speed > blade arrangement. The optimal simulation parameters were a 0.4 m/s forward speed, a 1700 r/min blade rotational speed, and a straight–curved blade arrangement, yielding a simulated cutting rate of 97.60%. Furthermore, field tests demonstrated that under these optimal parameters, influenced by complex paddy conditions and natural plant lodging, the actual average cutting rate was 91.39%. The machine exhibited excellent passability and pulverizing performance, thoroughly satisfying the requirements of agronomic and agricultural machinery integration.

Keywords: male parent cutting; hybrid rice; flail-blade type; pulverizing and returning to field; parameter optimization

Check for updates

Academic Editor: Ju-Seok Nam

Received: 17 July 2026
Revised: 15 August 2026
Accepted: 21 August 2026
Published: 26 August 2026

Copyright: © 2026 by the authors. Licensee MDPI, Basel, Switzerland. This article is an open access article distributed under the terms and conditions of the Creative Commons Attribution (CC BY) license.

1. Introduction

Hybrid rice seed production typically employs narrow-row intersecting planting patterns [1]. This specific agricultural scenario creates certain spatial limitations, requiring equipment to have a relatively narrow working width to avoid accidental injury to adjacent maternal plants [2]. Within this context, the timely removal of male parent rows is one of the key agronomic measures to improve seed yield and quality [3]. If the male parents are not removed promptly after the heading and flowering stages, they will compete

with the female parents (maternal plants) for light, water, and nutrients, leading to a decline in the seed-setting rate [4,5]. Moreover, during the rice harvesting process, partial grains from the male parents can be easily harvested together with the female parents, causing seed contamination [6]. Therefore, the cutting of male parents in seed production fields must generally be completed after the heading and flowering stages [7]. In recent years, despite the maturation of hybrid rice technology [8], the mechanization level of rice male parent harvesting during the seed cultivation stage remains relatively low [9,10]. Currently, the removal of male parents in the rice breeding process still widely relies on manual operation [11–13], which is constrained by low operational efficiency, high labor intensity, and poor cutting consistency [14]. Existing harvesting machinery is mostly designed for mature rice and is difficult to adapt to the physiological characteristics of hybrid rice male parents at the late flowering stage, which include high stalk moisture content, high toughness, and susceptibility to lodging [15]. Furthermore, due to the complex topography [16,17], deep mud, and poor machine passability in paddy fields, frequent occurrences of missed cuts and the crushing of maternal plants happen during the male parent cutting process. Consequently, there is an urgent need to develop specialized male parent selective cutting equipment that meets the agronomic requirements of hybrid rice seed production, achieving integrated operations of male parent cutting and maternal plant protection. As a national strategic base for Nanfan breeding, Hainan particularly needs to improve the mechanization level of rice male parent cutting in the seed cultivation process. Therefore, research on rice male parent cutting machines is of significant importance.

Currently, research dedicated specifically to rice male parent cutting machines is relatively scarce. However, technologies for combine harvesters and straw returning machines are well-established, offering valuable references for the design of header feeding mechanisms. For example, the W230 combine harvester developed by John Deere (USA) is utilized for harvesting crops such as rice and rapeseed. Its integrated straw chopping device utilizes chopping flappers to effectively chop and spread the straw, demonstrating commendable pulverizing performance. Nevertheless, it is designed primarily for single- or double-row narrow operations, rendering it unsuitable for the specific spatial constraints of plot breeding operations [18]. Similarly, the AS 30 WeedHex weeder developed by AS-Motor (Germany), intended for small forage crops, employs motor-driven high-speed rigid brushes for cutting and crushing [19]. Due to its limited working width and the complex conditions of actual paddy fields, it is also inapplicable for plot breeding operations.

Despite this, some progress has been made in the development of specialized equipment for rice male parent removal. Liu Haopeng et al. [20] from Huazhong Agricultural University developed an intelligent pulverizing robot for hybrid rice male parents. The machine controls locomotion and cutting actions via gear meshing and motor drives, featuring an adjustable row spacing mechanism. However, it lacks adequate consideration of actual field conditions, leading to a high risk of accidental injury to the maternal plants, which restricts its application in plot breeding. Zhu Kongxin et al. [21] designed the 9QS8 silage harvester, which employs multi-layer rotary double cutter heads to sever target crops. This design exploits the rotary motion to draw crops directly into a central channel, simplifying the feeding and conveying structure. Yet, the resulting header is excessively bulky, making it incompatible with plot breeding requirements. Furthermore, the 4Q-1.3Z straw pulverizing and returning machine developed by Shandong Aolong Co., Ltd. exhibits robust pulverizing capabilities for rice, wheat, and corn stalks. However, its rear-mounted operational configuration significantly increases the likelihood of damaging maternal plants, ultimately rendering it unsuitable for hybrid rice plot breeding operations [22,23].

Overall, to accommodate the complex conditions of muddy paddy fields and satisfy strict agronomic requirements within a limited working width, a specialized key cutting

device was designed. Compared to the bulky equipment featuring independently powered rotary cutter heads or rigid brushes reported in the literature, this study proposes a planetary carrier cutting device. Crucially, the key cutting device is driven by the rotation of the main shaft, which brings the flail blade into inertial rotation up to a stopper bar; the flail blade itself does not have independent power, nor does it perform continuous independent circular rotation. This innovative mechanism is not only more compact but also perfectly adaptable to the 500 mm narrow-row spacing, ensuring robust operational stability. Therefore, the primary objective of this study is to develop a walk-behind self-propelled hybrid rice male parent pulverizing and cutting machine for hybrid rice male parent removal based on this novel mechanism, to optimize its critical operational parameters through discrete element method (DEM) simulation, and to comprehensively validate its practical performance and feasibility through field trials.

2. Materials and Methods

2.1. Agronomic Analysis of Rice Cultivation

During hybrid rice seed production, male and female parent plants are typically cultivated simultaneously. Through genetic selection, rice seeds with superior genetic traits—such as high yield, lodging resistance, and disease and pest resistance—are obtained. Therefore, an optimized agronomic planting scheme is crucial for producing high-quality seeds.

Taking the rice breeding and seed production base in Sanya, Hainan, as an example, there are two primary planting patterns, as shown in Figure 1. Figure 1a illustrates a 2:3 planting pattern in greenhouses, which consists of an alternating arrangement of 2 male parent rows and 3 female parent rows. The row spacing between the male and female parent rows is 30 cm, while the row spacing between adjacent male parent rows and between adjacent female parent rows is 20 cm. The plant spacing for both male and female parent plants is uniformly 15 cm. Figure 1b depicts a 2:8 planting pattern utilized in field plots, featuring an alternating arrangement of 2 male parent rows and 8 female parent rows. In this pattern, the row spacing between the male and female parent rows is 20 cm, with all other planting parameters remaining consistent with those of the 2:3 greenhouse planting pattern.

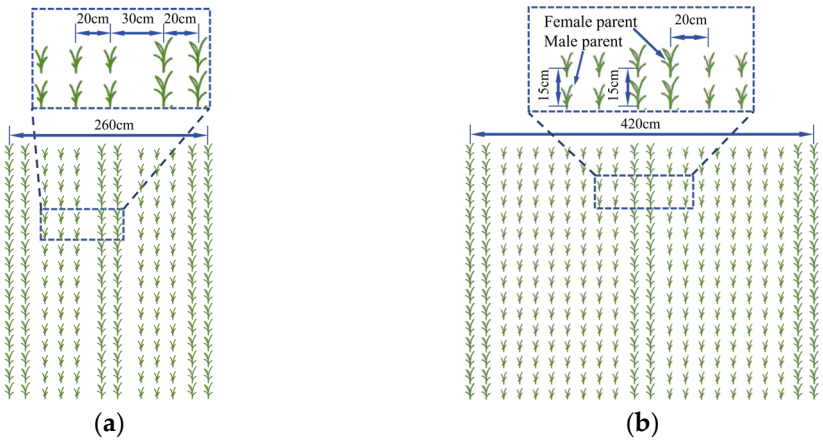


Figure 1. Planting patterns of hybrid rice: (**a**) greenhouse planting; (**b**) field plot planting.

To prevent seed contamination during the harvesting stage of hybrid rice seed production, male parent plants must be removed after pollination. However, due to the current low level of mechanization in rice breeding, male parent cutting is typically performed manually, resulting in severe labor intensity. Consequently, there is an urgent need to

design a walk-behind self-propelled cutting machine for the hybrid rice male parent to alleviate the labor burden.

2.2. Overall Structure and Working Principle

The overall structure of the walk-behind self-propelled hybrid rice male parent pulverizing and cutting machine is shown in Figure 2. It mainly consists of a crop dividing device, a depth-limiting device, a cutting device, an engine, mudguards, track wheels, and a hand-guided push rod. The entire machine adopts a narrow-body design with a maximum width of 550 mm to match the row spacing of hybrid rice male parents. A crawler chassis is designed to reduce ground-bearing pressure and adapt to muddy working environments in paddy fields, allowing for the single-pass completion of cutting, pulverizing, and returning the male parents to the field. The main parameters of the machine are shown in Table 1.

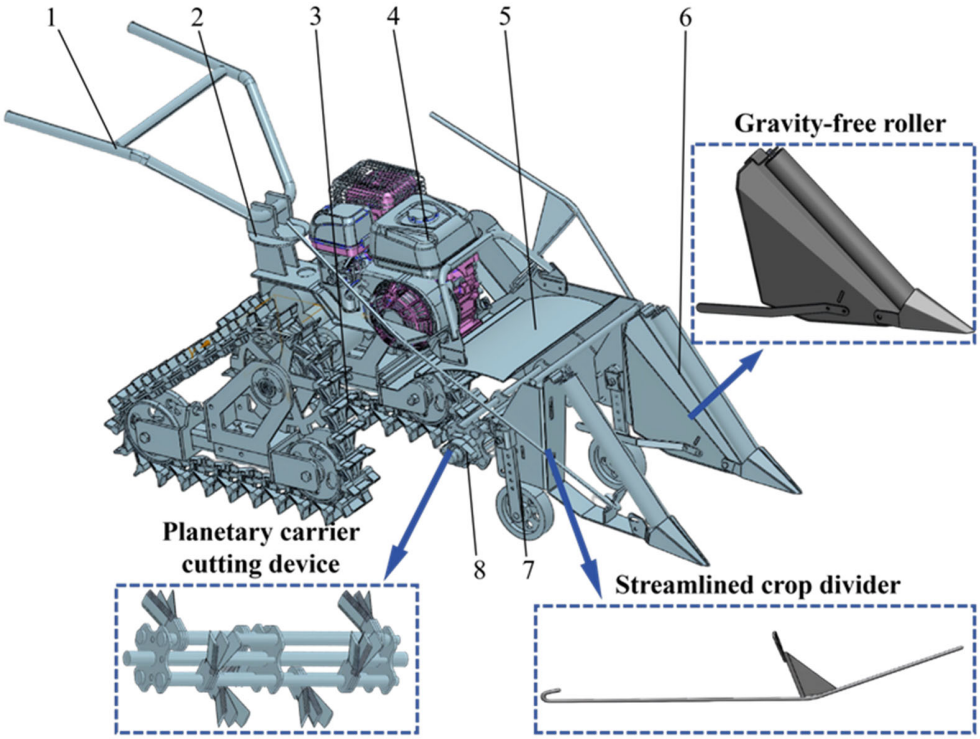


Figure 2. Overall structure of the walk-behind, self-propelled, hybrid rice male parent pulverizing and cutting machine. 1. Hand-guided push rod; 2. frame; 3. crawler chassis device; 4. diesel engine; 5. mudguard; 6. gravity-free crop dividing device; 7. depth-limiting wheel; 8. cutting device.

Table 1. Main parameters of the walk-behind, self-propelled, hybrid rice male parent pulverizing and cutting machine.

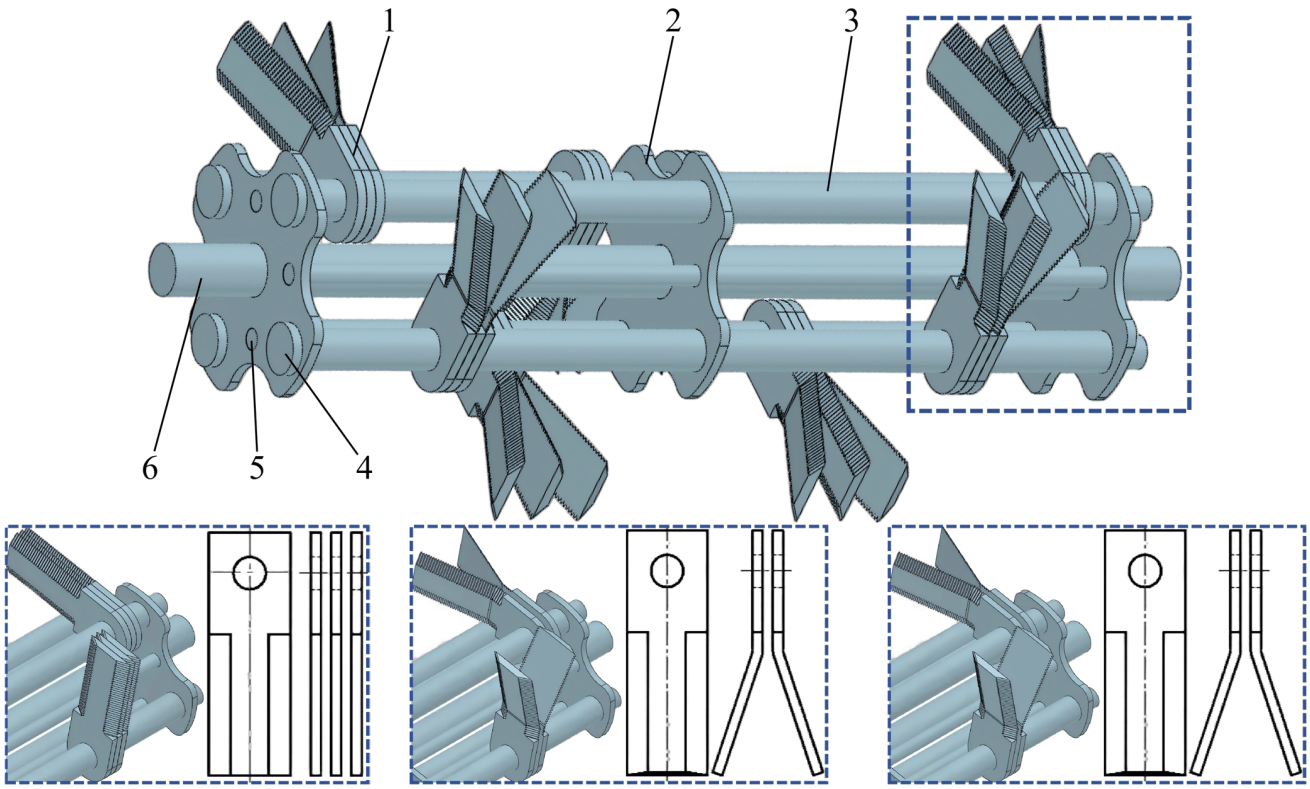
Parameter	Unit	Value
Overall dimensions	mm	1900 × 550 × 900
Machine weight	kg	240
Rated power	kW	3.6
Number of male parent rows cut	Row	1~2
Working efficiency	$hm^2 \cdot h^{-1}$	0.4~0.6

During operation, the operator guides the machine forward along the male parent rows using the hand-guided push rod. The engine power is transmitted to the main shaft of the cutting device via a belt transmission system, driving the flail-blade assembly to rotate at high speeds. The crawler walking system is independently driven, ensuring

sufficient traction and passability on soft paddy field surfaces. The crop dividers push aside the stalks of the adjacent maternal plants, reducing the maternal damage rate. The depth-limiting device controls the working position of the flail blades by adjusting the height of the profiling wheels, maintaining the stubble cutting height within 150 mm. The flail blades are deployed by the centrifugal force generated during high-speed rotation to cut off the male parent stalks, pulverizing them and returning them directly to the field.

2.3. Design of the Cutting Device and Flail-Blade Arrangements

The cutting device is the core working component of the machine, mainly composed of flail blades, the cutting device's main shaft, the flail blade's secondary shaft (planetary shaft), and flail-blade limit sleeves. Its function is to pulverize the hybrid rice male parents and return them to the field. The structure is shown in Figure 3. Given that the planting row spacing of the hybrid rice male parents is 20 cm, and the distance between the male and female parent rows is also 20 cm, the operation must satisfy the cutting of double rows of male parents while ensuring no damage to the female parents. Therefore, based on agronomic requirements, the working width of the cutting device is designed to be 500 mm.



(**a**) Uniform straight blade type (**b**) Symmetrical Y-type (**c**) Straight and symmetrical Y-type

Figure 3. Structure of the key cutting device and flail-blade arrangement scheme. 1. Replaceable flail blade. 2. Limit plate. 3. Limit sleeve. 4. Planetary shaft. 5. Stopper bar. 6. Main shaft.

The flail blades are made of 65Mn steel, which achieves a balance of high rigidity and toughness after quenching and tempering treatments. The four flail-blade shafts are evenly distributed on the circumference of the main shaft (diameter 50 mm). Limit sleeves are designed to prevent interference between adjacent flail blades, which would otherwise affect the quality of operation. A stopper bar (limit rod) is added between adjacent flail-blade shafts. During the high-speed rotation of the flail blades, this stopper bar not only constrains the swing amplitude of the blades to maintain sufficient cutting rigidity for

effective pulverization of the male parent plants, but also prevents mutual collision and interference between adjacent blades.

During the operation of the rice male parent cutting machine, influenced by factors such as vibration, noise, and rigid impact, different flail-blade arrangements have varying effects on cutting performance. To investigate the effect of blade arrangement on cutting performance, under the condition that the working width is fixed at 500 mm and the total number of flail blades is fixed at 24, three arrangement schemes were designed for comparative analysis: the first is a parallel arrangement of three straight flail blades (uniform straight blade type), with an arrangement density $\lambda_1 = 0.48$ blades/cm; the second is a symmetrical arrangement of two Y-shaped flail blades (symmetrical Y-type), with an arrangement density $\lambda_2 = 0.32$ blades/cm; and the third is the addition of a straight flail blade between symmetrically arranged Y-shaped flail blades (straight and symmetrical Y-shaped blade combination type), with an arrangement density $\lambda_3 = 0.40$ blades/cm as shown in Figure 3.

2.4. Kinematic and Force Analysis

In the cutting device, the motion trajectory of the flail blades is realized by the rotation of the main shaft driving the planetary shaft. During the startup and stopping phases, the action of centrifugal force causes the flail blades to undergo a certain degree of autorotation. The force analysis is shown in Figure 4. Therefore, prior to commencing cutting operations, it is necessary to wait until the main shaft of the cutting device reaches a stable operational state.

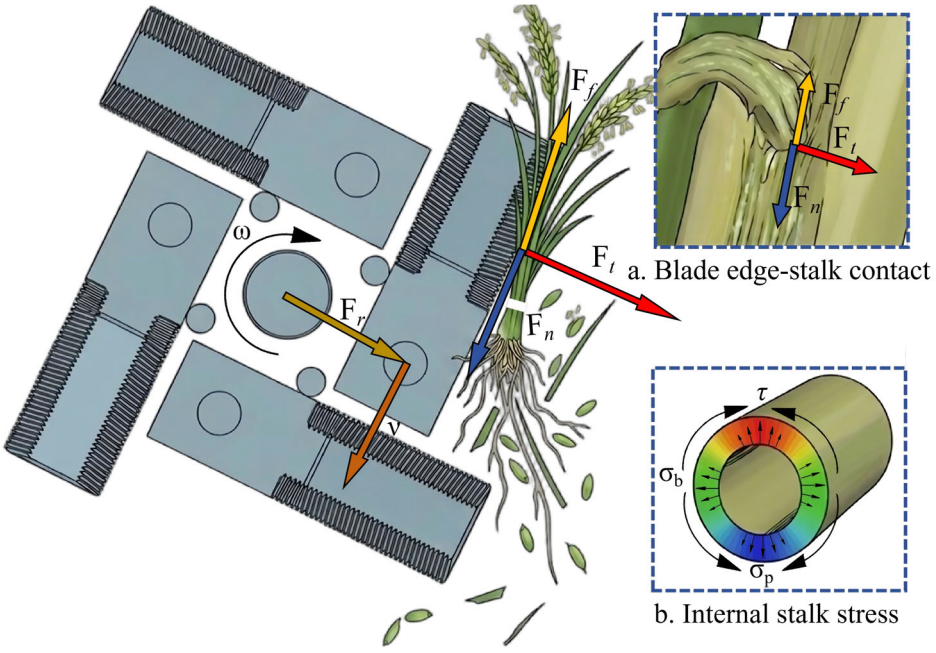


Figure 4. Force analysis diagram of the rotating cutting blade and the rice plant.

When the flail blades rotate to cut the rice stalks, the tangential velocity of the blade, v, must exceed the critical cutting velocity [24], generally requiring a tangential velocity of no less than 25 m/s. Assuming the flail-blade rotation radius is $R = 0.15$ m, the minimum rotational speed requirement is calculated as:

$$n_{min} = \frac{60v_c}{2\pi R} \quad (1)$$

where R is the rotational radius of the flail blade (m), and v_c is the linear velocity of the cutting blade (m/s).

Referring to the Agricultural Machinery Design Manual and comprehensively considering the control of machine vibration and noise, the theoretical minimum required rotational speed n_{min} is calculated to be approximately 1592 r/min according to Equation (1). However, this theoretical calculation relies solely on the ideal linear cutting velocity of the blade edge. During actual operation, the cutting mechanism involves a complex dynamic interaction where the planetary carrier generates a significant dragging force on the stalks as the machine advances. Due to this compounded force, effective stalk severing can still be achieved even when the rotational speed falls slightly below the theoretical linear threshold. Furthermore, to rigorously observe the actual cutting behavior, identify potential performance deterioration near this critical point, and validate the effect of the dragging force, the lower limit for the orthogonal experiment was intentionally set to 1500 r/min. This deliberate setting forms a scientific experimental gradient with the 1600 r/min and 1700 r/min levels.

To ensure that the cutting blades operate smoothly and steadily, dynamic balance during motion must be guaranteed. According to agricultural machinery manuals, when the number of blade groups is 8, the following equations must be satisfied:

$$\begin{cases} I_{xz} = \sum(n-i)sin\alpha_i = 0 \\ I_{yz} = \sum(n-i)cos\alpha_i = 0 \end{cases} \quad (2)$$

where n is the number of blade seat groups on the cutter shaft and α is the angle of the blade seat (°).

Given that the angle between adjacent flail-blade shafts of the pulverizing machine is 86.34°, the dynamic balance condition for the three-blade arrangement types is satisfied according to Equation (2). This result is consistent with theoretical analysis, and this angle is adopted as the design parameter for the blade arrangement of this machine.

As the machine advances, the absolute velocity of the blade is mainly the synthesis of the machine's forward speed and the rotary motion of the cutter shaft. Its motion trajectory is a trochoid, as shown in Figure 5. To ensure that the cutting device can move smoothly in the paddy field, improve the male parent cutting effect, and avoid the bulldozing phenomenon, a kinematic analysis of the cutting device was conducted.

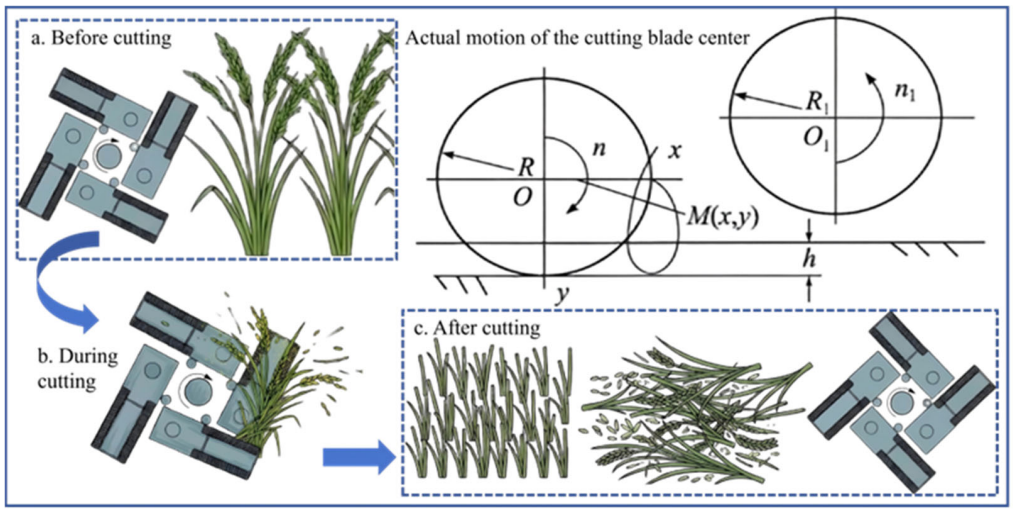


Figure 5. Kinematic and visual analysis of the cutting blade trajectory.

According to the equations of trochoid motion:

$$\begin{cases} x = R\,sin(\omega t) + v_0 t \\ y = R[1 - cos(\omega t)] \end{cases} \tag{3}$$

where R is the rotational radius of the flail blade (m), ω is the angular velocity of the cutter shaft (rad/s), v_0 is the forward speed of the machine (m/s), and t is the time (s).

To ensure that the trajectories of adjacent flail blades overlap effectively and avoid missed cuts, the overlap amount, δ, of adjacent blade cutting trajectories must satisfy:

$$\delta = \frac{v_0}{n \cdot z} \leq \Delta \tag{4}$$

where n is the rotational speed of the cutter shaft (r/min), Z is the number of flail blades in the same row, and δ is the maximum allowable missed-cut spacing (set to 10 mm).

2.5. Simulation Model Establishment

To investigate the interaction rules among key parameters such as cutter shaft speed, forward speed, blade arrangement, and the stalks of rice male parents, the discrete element method was employed to establish a rice male parent model, as shown in Figure 6. The EDEM 2024 software was used to conduct a simulation analysis of the cutting process of the rice male parent stalks by the flail blades [25–28].

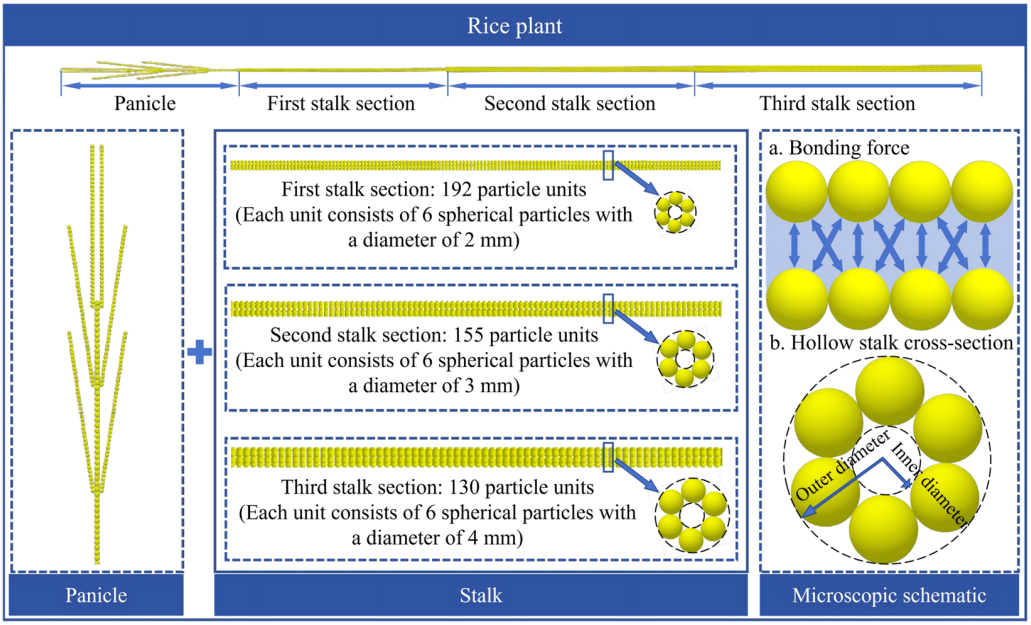


Figure 6. Discrete element model of the male parent plant of hybrid rice.

According to the relevant literature, the shear strength of crop stalks is significantly greater than that of the leaves [29]. Preliminary survey data and agronomic-machinery integration requirements also indicate that the male parent leaves are extremely flexible and their connection to the stalk is weak [30–32]. Therefore, the impact of the leaves on the blade-stalk contact load and the overall fracture mode during the cutting process is negligible. To simplify the complex mechanical interactions between the cutting device and the crop and to optimize the simulation computational time, the leaves were excluded from the model. Furthermore, because the tensile stress of the stalks is considerably higher than that of the leaves, any potential winding phenomenon around the cutter shaft or stopper bar would be primarily caused by the stalks rather than the easily sheared leaves.

Consequently, during the construction and simulation of the DEM model, this study focuses primarily on the collision, shearing, and fracture mechanical behaviors between the flail blades and the rice male parent stalks.

2.5.1. Particle Contact Mechanics and Fracture Model

To accurately reflect the mechanical properties of the male parent rice stalks, particularly their hollow structure, a multistage hollow stalk model was constructed. As illustrated in Figure 7, the particles situated between two sets of rigid rings correspond one-to-one, forming parallel bonds that transmit forces and moments at the contact points.

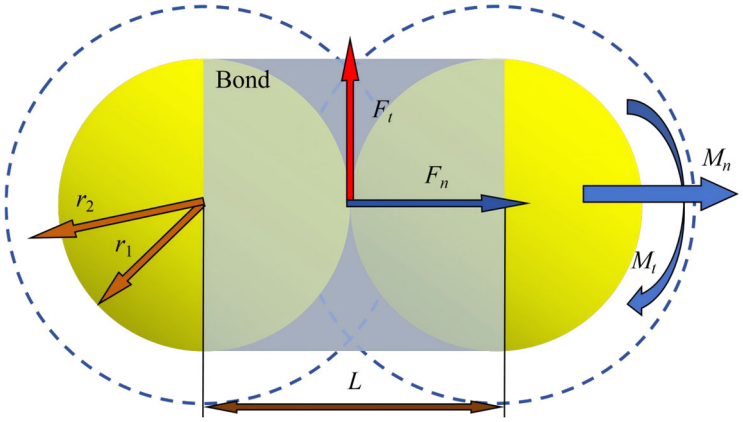


Figure 7. Schematic diagram of particle bonding.

Where, r_1 is the physical radius of the particle (mm); r_2 is the bond radius (mm); L is the distance between the two particles (mm); F_n and F_t are the normal and tangential forces of the bond (N); and M_n and M_t are the normal and tangential moments of the bond (N·m).

The cutting process of the male parent stalks by the inertial flail blades is essentially the accumulation of stress leading to bond breakage. To simulate this mechanical behavior, the parallel bond between the two particle rings is treated as a hollow Bernoulli beam. According to the mechanics of materials, the normal stiffness (k_n) and tangential stiffness (k_τ) of the ring-section beam per unit area can be expressed as follows:

$$\begin{cases} k_n = \frac{E_p}{L} \\ k_\tau = \frac{G_p}{L} \end{cases} \tag{5}$$

where E_P is the elastic modulus of the hollow particle (Pa); G_P is the shear modulus of the hollow particle (Pa); and L is the distance between the centers of two hollow particles (m).

When the particle shape and accumulation are fixed, the macroscopic Poisson's ratio (μ) is related to the stiffness ratio. Consequently, the normal-to-shear stiffness ratio of the hollow particles is established to be equal to the actual elastic-to-shear modulus ratio:

$$\frac{k_n}{k_\tau} = \frac{E}{G} = 2(1+\mu) \tag{6}$$

where E and G are the actual elastic modulus and shear modulus of the rice male parent, respectively (in Pa). The overall normal stiffness of the internodes ($k_n{}^r$) is determined by the series connection of parallel keys between N rings, expressed as:

$$k_n = \frac{(N-1)k_n^r}{A_v} \tag{7}$$

where A_v is the cross-sectional area of the hollow stem model (m^2).

During the cutting operation, the flail blades driven by the inertia of the main shaft generate violent impacts on the stalks. When either the normal force or the tangential force at the contact point reaches its maximum value, the parallel bond breaks, simulating the macroscopic fracture of the stalk. The critical normal stress (σ_{max}) and critical shear stress (τ_{max}) that dictate this bond breakage are determined by the maximum tensile force ($F_n{}^{max}$) and maximum shear force ($F_\tau{}^{max}$) relative to the actual cross-sectional area:

$$\begin{cases} \sigma_{max} = \frac{F_n^{max}}{A_v} \\ \tau_{max} = \frac{F_\tau^{max}}{A_v} \end{cases} \quad (8)$$

2.5.2. Setting of Simulation Parameters

The main shaft and planetary shafts of the cutting device are made of 45Mn steel, and the cutting blades are made of 65Mn steel. Based on preliminary research, initial experiments, and the relevant literature, the simulation parameters were set as shown in Table 2.

Table 2. Material properties and parameters.

Parameter	Unit	Value
Poisson's ratio of rice male parent		0.35
Shear modulus of rice stalk	Pa	1.8×10^6
Density of rice male parent	$kg \cdot m^{-3}$	215
Poisson's ratio of 65Mn steel		0.3
Shear modulus of 65Mn steel	Pa	7.8×10^{10}
Density of 65Mn steel	$kg \cdot m^{-3}$	7850
Stalk-stalk restitution coefficient		0.28
Static friction coefficient between rice stalks		0.38
Dynamic friction coefficient between rice stalks		0.30
Stalk-steel restitution coefficient		0.37
Static friction coefficient between rice stalk and 65Mn steel		0.34
Dynamic friction coefficient between rice stalk and 65Mn steel		0.23

2.5.3. Experimental Design and Factor Levels for Hybrid Rice Male Parent Cutting

To investigate the effects of key parameters—such as cutter shaft rotational speed, forward speed, and blade arrangement—on the cutting rate of the hybrid rice male parent, single-factor simulation experiments were conducted. These experiments were designed based on preliminary survey data, and the requirements for the integration of agricultural machinery and agronomy are detailed in Table 3.

Table 3. Experimental factors and levels.

Level	Forward Speed $m \cdot s^{-1}$	Flail-Blade Speed $r \cdot min^{-1}$	Blade Combination Arrangement
−1	0.4	1500	a. Uniform straight blade type
0	0.5	1600	b. Symmetrical Y-type
1	0.6	1700	c. Straight and symmetrical Y-type

A three-factor, three-level orthogonal experimental design was adopted, and simulation analysis was conducted using EDEM 2024 software.

2.6. Field Test Methodology

To further verify the reliability and the optimization results of the operating parameters for the key cutting device obtained from the EDEM 2024 simulation, field trials were conducted using the optimized parameters on a walk-behind self-propelled hybrid rice

male parent pulverizing and cutting machine, as shown in Figure 8. The field validation was performed in May 2026 at the Batou Base experimental field of Hainan University in Sanya, Hainan Province. The primary experimental equipment and instruments used included the walk-behind self-propelled hybrid rice male parent cutting machine, electronic sensors, vernier calipers, and tape measures. The tested rice variety was 'Shuyounuo No. 81' with an average moisture content of 74.6%.

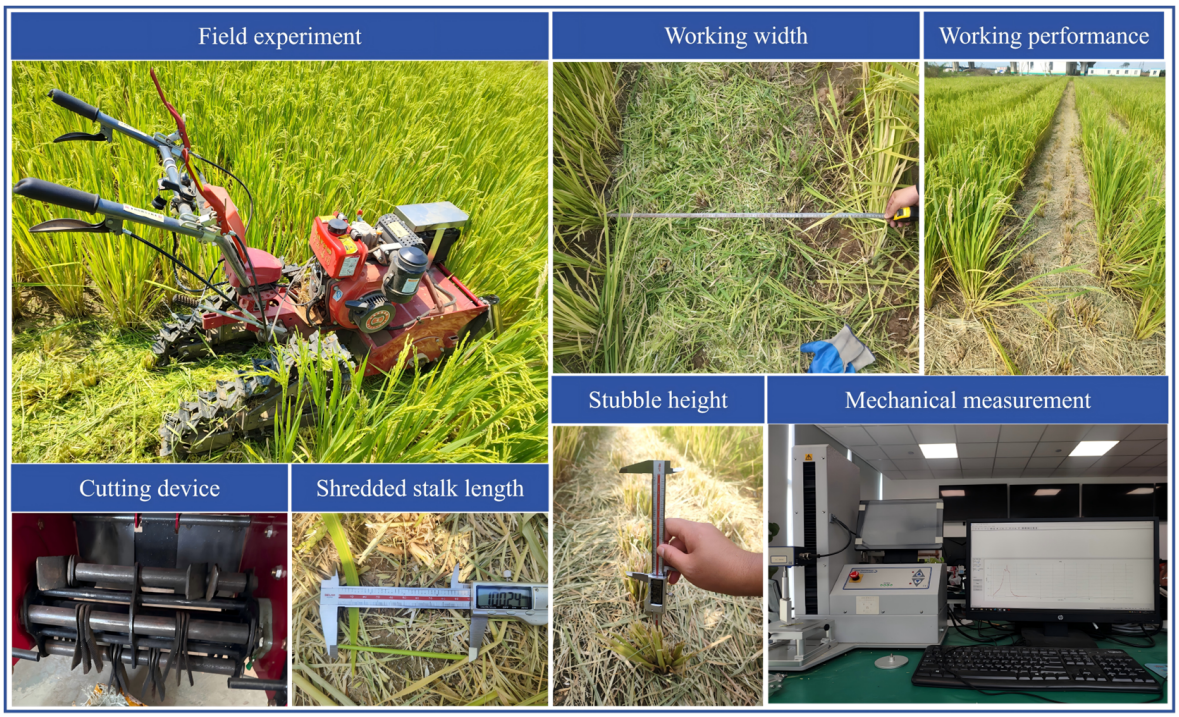


Figure 8. Field-trial equipment.

The actual rotational speed of the cutting device and the machine's forward speed were measured using sensors, while the stubble cutting height of the male parent was measured using vernier calipers and tape measures. The primary evaluation index, the cutting rate of the male parent (C_r), is mathematically defined as follows:

$$C_r = \frac{N_c}{N_t} \times 100\% \tag{9}$$

where N_c is the number of successfully shredded male parent plants (stubble height $\leq$ 15 cm), and N_t is the total number of male parent plants within the operation area. The maternal plant damage rate per 300 rice plants was also calculated as a key evaluation index. To ensure accuracy and mitigate data errors caused by inconsistent planting methods at the field ends compared to the field center, the rice at the field ends was cut first to guarantee consistency among the tested rice plants in the central area. Five repeated field tests were conducted, and the average value was adopted as the final experimental index.

3. Results

3.1. Simulation Results and Parameter Optimization

The experiments utilized EDEM 2024 software for simulation analysis [33]. The visualized experimental results under different factors and levels were recorded, as shown in Figure 9.

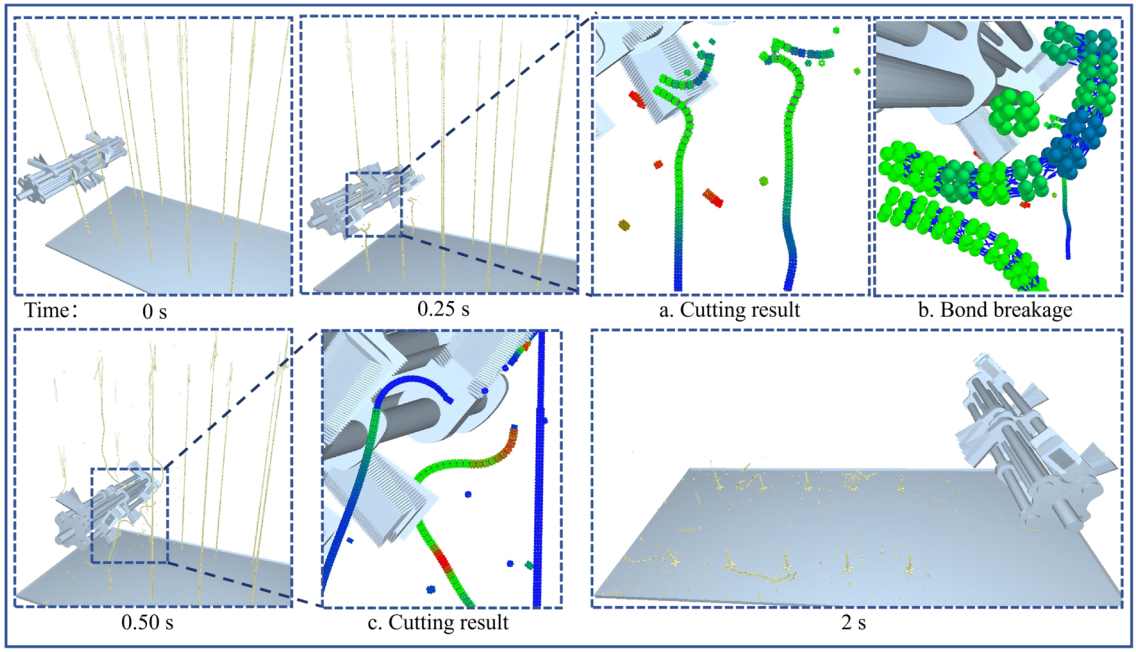


Figure 9. Visualization of cutting effects at different times during simulation experiments. (**a**) Close-up of cutting effect at 0.25 s. (**b**) Close-up of bond breakage at 0.25 s. (**c**) Close-up of cutting effect at 0.50 s.

During the simulation cutting process, in combination with agronomic-machinery integration theory, a stubble cutting height of ≤15 cm was used as an important criterion for determining the cutting rate [34,35]. The simulation effects at each stage under different levels were documented.

3.1.1. Experimental Design and Analysis

The experimental scheme and results are presented in Table 4. The primary experimental factors, denoted as A, B, and C, represent the forward speed, flail-blade rotational speed, and blade arrangement, respectively. The cutting rate of the hybrid rice male parent was chosen as the evaluation index.

Table 4. Experimental design and results of 3 factors and 3 levels.

No.	Forward Speed ($m \cdot s^{-1}$)	Flail-Blade Speed ($r \cdot min^{-1}$)	Blade Combination Arrangement	Cutting Rate (%)
1	0.4	1700	a	95.00
2	0.4	1700	b	96.33
3	0.4	1700	c	97.67
4	0.6	1700	c	93.56
5	0.4	1500	a	91.11
6	0.4	1600	a	93.00
7	0.5	1500	a	90.00
8	0.5	1500	b	91.22
9	0.5	1500	c	92.44
10	0.5	1600	a	91.44
11	0.4	1600	b	94.33
12	0.5	1600	b	92.67
13	0.6	1600	a	90.00
14	0.6	1700	a	91.22
15	0.5	1600	c	93.89

Table 4. *Cont.*

No.	Forward Speed ($m \cdot s^{-1}$)	Flail-Blade Speed ($r \cdot min^{-1}$)	Blade Combination Arrangement	Cutting Rate (%)
16	0.6	1700	b	92.33
17	0.4	1500	b	92.33
18	0.6	1600	c	92.11
19	0.5	1700	a	92.89
20	0.5	1700	b	94.11
21	0.5	1700	c	95.33
22	0.6	1600	b	91.00
23	0.6	1500	a	88.78
24	0.4	1600	c	95.67
25	0.4	1500	c	93.67
26	0.6	1500	b	89.78
27	0.6	1500	c	90.89

Based on the experimental design and the results in Table 4, a range analysis was first conducted. The results are shown in Table 5.

Table 5. Range analysis.

No.	Forward Speed ($m \cdot s^{-1}$)	Flail-Blade Speed ($r \cdot min^{-1}$)	Blade Combination Arrangement
K_{1j}	849.11	820.22	823.44
K_{2j}	833.99	834.11	834.1
K_{3j}	819.67	848.44	845.23
k_{1j}	94.35	91.14	91.49
k_{2j}	92.67	92.68	92.68
k_{3j}	91.07	94.27	93.91
R_j	3.28	3.13	2.42
Order of significance		A > B > C	
Optimal level		A1, B3, C3	

As seen in Table 5, $R_A > R_B > R_C$. The primary and secondary order of influence of each factor on the cutting rate of hybrid rice male parents is A > B > C. That is, forward speed has the greatest impact on the cutting rate, making it the most critical factor, followed by the flail-blade rotational speed, while the blade arrangement has a relatively minor effect. From the perspective of agronomic-machinery integration, a slower forward speed and higher flail-blade speed yield better cutting results. Simultaneously, the third blade arrangement (straight and symmetrical Y-shaped blade combination type) is more suitable for cutting rice male parents.

Next, an ANOVA considering the main factors was conducted, and the results are shown in Table 6.

Table 6. Results of variance analysis for the main factors.

Variance Source	Sum of Squares	Degree of Freedom	Mean Square	*F*-Value	*p*-Value
Model	118.79	6	19.80	219.07	<0.0001
A	48.15	1	48.15	532.79	<0.0001
B	44.24	1	44.24	489.55	<0.0001
C	26.38	1	26.38	291.87	<0.0001
A^2	0.0119	1	0.0119	0.1311	0.7211
B^2	0.0036	1	0.0036	0.0397	0.8441
C^2	0.0041	1	0.0041	0.0453	0.8337
Residual	1.81	20	0.0904		
Cor Total	120.60	26			

The ANOVA results indicate that the main factors—forward speed, flail-blade rotational speed, and blade arrangement—all have an extremely significant impact on the cutting rate of the rice male parents ($p < 0.001$). Since the insignificant quadratic terms have been eliminated, the regression equation fits well and is expressed as Equation (10):

$$y_1 = 73.3674 - 16.3556x_1 + 0.0156778x_2 + 1.21056x_3 \quad (10)$$

Subsequently, an ANOVA that considered interaction effects was conducted. The results are presented in Table 7.

Table 7. Analysis of variance, including interaction effects.

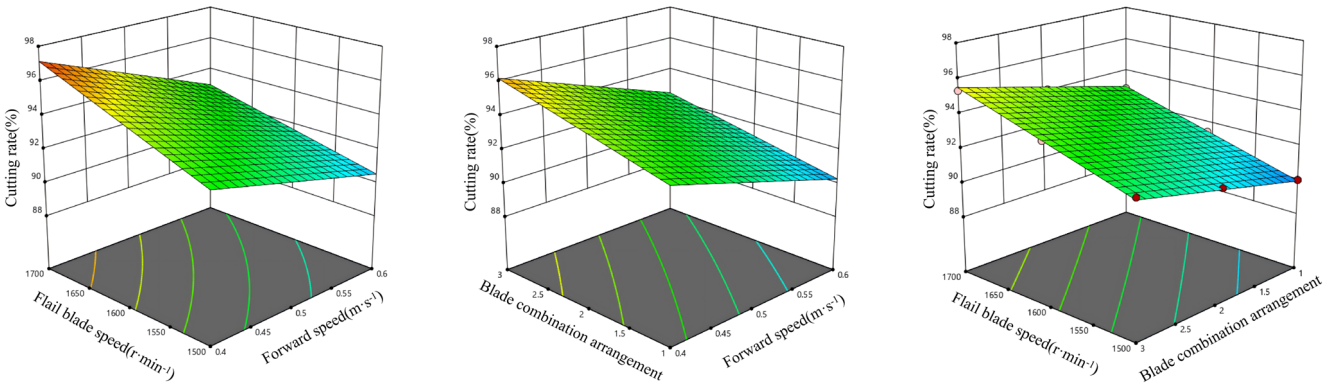
Variance Source	Sum of Squares	Degree of Freedom	Mean Square	*F*-Value	*p*-Value
Model	120.42	6	20.07	2271.91	<0.0001
A	48.15	1	48.15	5450.54	<0.0001
B	44.24	1	44.24	5008.16	<0.0001
C	26.38	1	26.38	2985.92	<0.0001
AB	1.49	1	1.49	168.79	<0.0001
AC	0.1496	1	0.1496	16.94	0.0005
BC	0.0096	1	0.0096	1.09	0.3088
Residual	20	0.0088			
Cor Total	26				

As shown in Table 7, the interaction between forward speed and flail-blade rotational speed has an extremely significant effect on the cutting rate. The interaction between forward speed and blade arrangement has a significant effect, whereas the interaction between flail-blade rotational speed and blade arrangement is not significant. Removing the non-significant interaction yields the refined regression equation below:

$$y_1 = 44.0507 + 42.2778x_1 + 0.0333028x_2 + 1.76889x_3 - 0.03525x_1x_2 - 1.11667x_1x_3 \quad (11)$$

3.1.2. Response Surface Analysis of Interaction Effects

Based on the regression equation, a response surface analysis was generated using Design-Expert 13, as illustrated in Figure 10.



(**a**) A–B (**b**) A–C (**c**) B–C

Figure 10. Effects of interactions among various factors on the male parent cutting rate. (**a**) A–B interaction. (**b**) A–C interaction. (**c**) B–C interaction.

As shown in Figure 10a, regarding the interaction between flail-blade speed and forward speed: as the flail-blade speed increases and the forward speed decreases, the cutting effect on the male parent improves, indicating a negative correlation. Figure 10b indicates that for the third blade arrangement (straight–curved combination), a lower

forward speed yields better cutting results. Figure 10c shows that the interaction between flail-blade speed and blade arrangement is not significant.

3.1.3. Optimization Analysis of Simulation Results

To determine the optimal operational parameters of the cutting device, the established regression model was optimized with constraints on forward speed, flail-blade rotational speed, and blade arrangement. Using Design-Expert 13, the optimal theoretical values obtained were a forward speed of 0.4 m/s, flail-blade rotational speed of 1700 r/min, and the straight–curved blade arrangement. Under these conditions, the theoretical cutting rate reached 97.60%, fulfilling agronomic requirements.

$$\begin{cases} maxy(x_1, x_2, x_3) \\ s.t. \begin{cases} 0.4\ \text{m/s} \le x_1 \le 0.6\ \text{m/s} \\ 1500\ \text{r/min} \le x_2 \le 1700\ \text{r/min} \\ a \le x_3 \le c \end{cases} \end{cases} \tag{12}$$

3.2. Field Test Results

Based on the optimal simulated values (forward speed of 0.4 m/s, flail-blade speed of 1700 r/min, straight–curved arrangement), five replicate tests were performed. The results are shown in Table 8.

Table 8. Field test results.

No.	Forward Speed ($m \cdot s^{-1}$)	Flail-Blade Speed ($r \cdot min^{-1}$)	Blade Combination Arrangement	Cutting Rate (%)
1	0.4	1700	c	91.47
2	0.4	1700	c	90.07
3	0.4	1700	c	91.73
4	0.4	1700	c	92.27
5	0.4	1700	c	91.40
k				91.39
CV				0.89

Applying the optimal parameters (0.4 m/s, 1700 r/min, straight + Y arrangement) to the physical prototype, five field test replicates yielded actual cutting rates of 91.47%, 90.07%, 91.73%, 92.27%, and 91.40%. Statistical analysis revealed an average actual cutting rate of 91.39%, with a standard deviation (*SD*) of 0.81 and a coefficient of variation (*CV*) of 0.89%. This extremely low coefficient of variation strongly demonstrates that the equipment maintains exceptionally high operational stability and reliability even under the complex and dynamic conditions of actual paddy fields, thoroughly proving the equipment's feasibility for agricultural deployment.

4. Discussion

While the machine demonstrated robust passability and pulverizing capability, there was a 6.21% discrepancy between the actual field cutting rate (91.39%) and the idealized simulation rate (97.60%).

(1) The simulation model assumed an ideally flat, rigid ground surface, whereas actual paddy fields have varying mud depths and uneven soil bearing capacity. The crawler chassis experiences local sinking or slight slipping during travel, causing dynamic pitch and roll of the machine body. This dynamic posture variation causes continuous fluctuations in the actual ground clearance of the cutting device, resulting in some male parent stalks

slipping outside the effective cutting width and height zones, which directly increases the missed cutting rate.

(2) The EDEM 2024 simulation utilized a uniformly upright, flexible plant model. However, in real Nanfan seed production fields, the male parent stalks at the late flowering stage have high moisture content and high shear resistance. Influenced by the field microclimate, numerous plants exhibit natural tilting, lodging, or cross-growth with maternal plants. When the high-speed flail blades strike non-upright, high-toughness stalks, a "dragging" effect rather than a crisp "cutting" effect often occurs, reducing the success rate of a single-pass pulverization.

(3) During actual paddy operations, the high-speed rotating flail-blade assembly inevitably kicks up mud, water weeds, and crushed stalk debris. These impurities adhere to the flail blades and the main shaft, dulling the effective cutting edge of the blades, disrupting the dynamic balance of the cutter shaft, and adding extra load. Additionally, the continuous vibration of the engine and transmission belt under heavy load causes the actual cutting motion trajectory of the blade edge to deviate further from the theoretical trochoid trajectory.

Compared to existing agricultural equipment, the proposed machine exhibits distinct structural and performance advantages in narrow-row hybrid rice seed production scenarios. For instance, while the intelligent pulverizing robot designed by Liu et al. utilizes gear and motor drives for cutting, it lacks sufficient maternal plant protection mechanisms in complex field conditions, leading to a high risk of accidental injury. Similarly, traditional large-scale straw returning machines, such as the 4Q-1.3Z model, possess strong pulverizing capabilities, but their bulky rear-mounted headers are fundamentally incompatible with plot breeding, often causing severe crushing damage to adjacent rows. The machine proposed in this study successfully overcomes these limitations by coupling an inertial flail-blade mechanism with a gravity-free crop dividing device. This structural synergy not only achieves a highly stable actual cutting rate of 91.39% but also physically shields the maternal plants, demonstrating superior pulverizing thoroughness and completely preventing mechanical damage to the female parents.

From a techno-economic perspective, the mechanization of male parent removal offers profound benefits over traditional manual methods, which are notoriously labor-intensive, inefficient, and heavily constrained by poor cutting consistency. Currently, agricultural mechanization is a critical pathway to improving efficiency in seed production. The developed machine addresses this bottleneck directly by operating at an impressive working efficiency of 0.4~0.6 hm^2/h while relying on a highly economical 3.6 kW rated power diesel engine. Assuming a standard manual labor efficiency of roughly 0.02~0.03 hm^2/h per worker under similar muddy conditions, a single operator utilizing this walk-behind machine can replace the intensive labor of approximately 20 manual workers. This drastic reduction in labor dependency and time costs, combined with minimal fuel consumption, underscores the immense economic viability and practical application value of this equipment for large-scale Nanfan hybrid rice seed cultivation.

5. Conclusions

(1) To address the critical challenges of seed contamination, narrow-row mechanized cutting difficulties, and potential damage to maternal plants in muddy paddy fields, a walk-behind self-propelled pulverizing and cutting machine for hybrid rice male parents was developed. The machine integrates three essential modules: a crawler walking mechanism for high passability, a gravity-free crop dividing device, and an innovative cutting device. The cutting device operates on a principle where the high-speed rotation of the main shaft drives the flail blades into inertial autorotation. The flail blades are not independently

powered, and their maximum swing amplitude is physically constrained by a stopper rod. This structural synergy guarantees a 500 mm working width for efficient one-time stalk pulverization, while working in tandem with the crop dividing device to safely push aside adjacent maternal plants, effectively preventing accidental mechanical injury and subsequent seed contamination.

(2) DEM simulations via EDEM 2024 software identified the optimal operating parameters for maximum efficiency: a forward speed of 0.4 m/s, a flail-blade rotational speed of 1700 r/min, and a straight–curved blade arrangement. In the simulated environment, this combination yielded a cutting rate of 97.60%.

(3) Field experiments validated the design's practical viability. Despite a 6.21% deviation caused by the harsh dynamic variables of actual paddy environments (e.g., mud variations and plant lodging), the machine achieved a stable 91.39% cutting rate under optimal parameters. The equipment thoroughly satisfies the integrated requirements of agricultural machinery and agronomy for hybrid rice seed production.

(4) Future research will focus on upgrading the machine with visual navigation and autonomous driving technologies to achieve fully unmanned operation, thereby further alleviating the labor shortage in Nanfan breeding. Furthermore, comprehensive, multi-season field evaluations directly involving local farmers will be conducted to rigorously assess the machine's durability, operational user-friendliness, and long-term economic impact in real-world agricultural applications.

Author Contributions: The study presented here was carried out collaboratively by all authors. Conceptualization, R.Y., H.Z., W.L., Y.Q. and Z.X.; methodology, H.Z., W.L., X.Z. and J.Z.; software, H.Z. and W.L.; validation, H.Z. and W.L.; formal analysis, H.Z. and W.L.; writing—original draft preparation, H.Z.; writing—review and editing, W.L.; funding acquisition, R.Y.; visualization, H.Z.; supervision, R.Y. and W.L.; project administration, R.Y. All authors have read and agreed to the published version of the manuscript.

Funding: This work was supported by the National Key Research and Development Program of China (Grant No. 2023YFD2000400) and the China Postdoctoral Science Foundation (Grant No. 2026M792650).

Data Availability Statement: The original contributions presented in this study are included in the article. Further inquiries can be directed to the corresponding author.

Acknowledgments: The authors gratefully acknowledge the administrative and technical support provided by Hainan University.

Conflicts of Interest: Zhuxin Xu is employed by Qingdao Plantech Mechanical Technology Co., Ltd. The remaining authors declare that the research was conducted in the absence of any commercial or financial relationships that could be construed as potential conflicts of interest.

Abbreviations

The following abbreviations are used in this manuscript.

ANOVA	Analysis of Variance
DEM	Discrete Element Method

References

1. Zheng, X.; Wei, F.; Cheng, C.; Qian, Q. A historical review of hybrid rice breeding. *J. Integr. Plant Biol.* **2024**, *66*, 532–545. [CrossRef]
2. Yan, Y.; Lei, B.; Hu, Y.; Wang, M.; Liu, D.; Chen, K.; Liu, H.; Tang, C.; Li, F.; Tang, N.; et al. Innovations in hybrid rice seed production: Integrating agronomy, mechanization, and biotechnology. *Plant Commun.* **2026**, *7*, 101931. [CrossRef]
3. He, L.; Luo, H.; Duan, M.; Kong, L.; Tang, X. Mechanized hybrid rice seed production: Planting density, the flight height of an unmanned aerial vehicle, fertilizer application, and the row-ratio of parents. *Agronomy* **2022**, *12*, 1572. [CrossRef]

4. Sims, L.; Pastor, J.; Lee, T.; Dewey, B. Nitrogen, phosphorus, and light effects on reproduction and fitness of wild rice. *Botany* **2012**, *90*, 876–883. [CrossRef]
5. Patnaik, G.P.; Thavaprakaash, N.; Sachin, S.S. Moisture stress at critical stages of rice (*Oryza sativa*) hampers grain yield and economics by inhibiting the growth and yield-forming traits. *Indian J. Agric. Sci.* **2025**, *95*, 1345–1350. [CrossRef]
6. Wang, X.; Zheng, H.; Tang, Q. Early harvesting improves seed vigour of hybrid rice seeds. *Sci. Rep.* **2018**, *8*, 11092. [CrossRef]
7. Xia, Y.; Tang, N.; Hu, Y.; Li, D.; Li, S.; Bu, X.; Yu, M.; Qi, S.; Yang, Y.; Zhu, H.; et al. A method for mechanized hybrid rice seed production using female sterile rice. *Rice* **2019**, *12*, 39. [CrossRef]
8. Liao, C.; Yan, W.; Chen, Z.; Xie, G.; Deng, X.W.; Tang, X. Innovation and development of the third-generation hybrid rice technology. *Crop J.* **2021**, *9*, 693–701. [CrossRef]
9. Gan, Q.; Zhou, R.; Yu, H.; Lin, C.X.; Teng, B.; Song, F.S.; Ni, D.H. A novel labor-saving strategy for hybrid rice seed production. *J. Integr. Agric. (JIA)* **2026**, *25*, 2623–2626. [CrossRef]
10. Min, S.H.I.; Paudel, K.P. Mechanization and efficiency in rice production in China. *J. Integr. Agric.* **2021**, *20*, 1996–2008. [CrossRef]
11. Huang, K.; Li, Y. Genetic editing of grain size genes enables fully mechanized hybrid rice breeding. *Nat. Plants* **2024**, *10*, 844–845. [CrossRef]
12. Deng, R.; Cheng, W.; Liu, H.; Hou, D.; Zhong, X.; Huang, Z.; Xie, B.; Yin, N. Automatic identification of sea rice grains in complex field environment based on deep learning. *Agriculture* **2024**, *14*, 1135. [CrossRef]
13. Deng, R.; Liu, W.; Liu, H.; Liu, Q.; Zhang, J.; Hou, M. Non-Destructive Measurement of Rice Spikelet Size Based on Panicle Structure Using Deep Learning Method. *Agronomy* **2024**, *14*, 2398. [CrossRef]
14. Huang, M.; Chen, G.; Chen, J.; Cao, F.; Li, Z.; Chen, Y.; Liu, L.; Zou, Y. Yield performance of inbred rice grown under labor-saving crop establishment methods. *Agron. J.* **2021**, *113*, 5126–5132. [CrossRef]
15. Sakran, R.M.; Ghazy, M.I.; Gaballah, M.M.; Hussein, F.A.; Aamer, S.M.; Ghazy, H.A.; Lamlom, S.F.; Abdelghany, A.M. Genetic variability in physiological and agronomic traits of newly developed rice lines under well-watered and water-deficit conditions. *BMC Plant Biol.* **2025**, *25*, 1291. [CrossRef]
16. He, Y.; Zhou, J.; Sun, J.; Jia, H.; Liang, Z.; Awuah, E. An adaptive control system for path tracking of crawler combine harvester based on paddy ground conditions identification. *Comput. Electron. Agric.* **2023**, *210*, 107948. [CrossRef]
17. Tu, T.; Luo, X.; Hu, L.; Chung, S.-O.; He, J.; Zhao, R.; Wang, P.; Chen, G.; Feng, D.; Yue, M.; et al. Methods and experiments for analysing hard-bottom layer changes and monitoring wheel sink depth in paddy fields. *Comput. Electron. Agric.* **2025**, *238*, 110760. [CrossRef]
18. Boroujeni, F.M.; Maleki, A. Fractal analysis of noise signals of Sampo and John Deere combine harvesters in operational conditions. *Arch. Acoust.* **2019**, *44*, 89–98. [CrossRef]
19. Pandey, H.S.; Tiwari, G.S.; Sharma, A.K. Design and development of an e-powered inter row weeder for small farm mechanization: E-powered inter row weeder for small farm mechanization. *J. Sci. Ind. Res. (JSIR)* **2023**, *82*, 671–682. [CrossRef]
20. Liu, H.; Ai, Y.; Yang, N.; Deng, Y.; Lin, Z.; Li, S.; Li, Z.; Zhou, R. An Intelligent Hybrid Rice Male Parent Pulverizing Robot. China Patent No. CN 214228964 U, 12 March 2021.
21. Zhu, K.; Ning, E.; Zhao, M.; Hu, G.; Wei, Z.; Jia, J. Virtual design and test of 9QS8 silage harvester based on Solidworks. *J. Agric. Mech. Res.* **2009**, *31*, 137–139.
22. Wang, J.; Zhao, W.; Liu, X.; Dai, F.; Shi, R.; Zhang, K.; Wang, X.; Zhang, W.; Liang, J. The Design and Testing of a Combined Operation Machine for Corn Straw Crushing and Residual Film Recycling. *Agriculture* **2025**, *15*, 916. [CrossRef]
23. Wang, S.; Pan, J.; Xiao, Q.; You, Z.; Li, J.; Gao, X.; Xie, S. Design of a deviation information detection mechanism for sugar beet harvesters based on agricultural machinery and agronomy integration. *Int. J. Agric. Biol. Eng.* **2026**, *19*, 120–131. [CrossRef]
24. Deshmukh, M.; Thakare, S.K.; Ghorade, R.B. Effect of cutting blade parameters on harvesting of sorghum stalks. *AMA Agric. Mech. Asia Afr. Lat. Am.* **2023**, *54*, 7–10.
25. Chen, G.; Wang, Q.; Li, H.; He, J.; Wang, X.; Zhang, X.; He, D. Experimental research on vertical straw cleaning and soil tillage device based on Soil-Straw composite model. *Comput. Electron. Agric.* **2024**, *216*, 108510. [CrossRef]
26. Patwa, A.; Ambrose, R.K.; Casada, M.E. Discrete element method as an approach to model the wheat milling process. *Powder Technol.* **2016**, *302*, 350–356. [CrossRef]
27. Leblicq, T.; Smeets, B.; Vanmaercke, S.; Ramon, H.; Saeys, W. A discrete element approach for modelling bendable crop stems. *Comput. Electron. Agric.* **2016**, *124*, 141–149. [CrossRef]
28. Chen, X.; Li, Y.; Sun, W.; Zhang, H.; Liu, S.; Wang, J.; Jing, L.; Song, Q. Discrete Element Method-Based Simulation for Rice Straw Comminution and Device of Parameter Optimization. *Appl. Sci.* **2026**, *16*, 1934. [CrossRef]
29. Zhang, L.; Ma, Z.; He, N.; Tang, Z.; Wang, C.; Zheng, W.; Wang, H.; Sui, G.; Gao, H.; Wang, L. Lodging resistance of Japonica hybrid rice plants studied in relation to mechanical and physicochemical characteristics. *Agronomy* **2025**, *15*, 699. [CrossRef]
30. Leblicq, T.; Vanmaercke, S.; Ramon, H.; Saeys, W. Mechanical analysis of the bending behaviour of plant stems. *Biosyst. Eng.* **2015**, *129*, 87–99. [CrossRef]

31. Ho, N.X.; Le, T.-T.; Nguyen, X.-S.; Nguyen, N.T.H. Combining experiments and DEM simulations for characterization of physical and mechanical properties of rice, glutinous rice, corn and sesame for discrete element modeling. *Part. Sci. Technol.* **2026**, 1–19. [CrossRef]
32. Robertson, D.J.; Smith, S.L.; Cook, D.D. On measuring the bending strength of septate grass stems. *Am. J. Bot.* **2015**, *102*, 5–11. [CrossRef]
33. Jia, H.; Deng, J.; Deng, Y.; Chen, T.; Wang, G.; Sun, Z.; Guo, H. Contact parameter analysis and calibration in discrete element simulation of rice straw. *Int. J. Agric. Biol. Eng.* **2021**, *14*, 72–81. [CrossRef]
34. Dai, Y.; Song, M.; Liu, Y.; Zhang, Y.; Zhu, J.; Peng, H. Effect of Stubble Height on Cadmium Removal Potential of Removed Straw. *Sustainability* **2025**, *17*, 7123. [CrossRef]
35. Yu, X.; Yang, G.; Zhang, Z.; Guo, Y.; Zheng, C.; Xu, L.; Yuan, S.; Xiong, D.; Peng, S. Cutting height of main crop has profound effects on cadmium but not arsenic concentration of ratoon crop in rice. *Field Crops Res.* **2023**, *302*, 109085. [CrossRef]

Disclaimer/Publisher's Note: The statements, opinions and data contained in all publications are solely those of the individual author(s) and contributor(s) and not of MDPI and/or the editor(s). MDPI and/or the editor(s) disclaim responsibility for any injury to people or property resulting from any ideas, methods, instructions or products referred to in the content.